

1 **Modeling soiling losses for rooftop PV systems in suburban areas with** 2 **nearby forest in Madrid**

3 Jesús Polo ^{1*}, Nuria Martín-Chivelet¹, Carlos Sanz-Saiz¹, Joaquín Alonso-Montesinos², Gabriel
4 López³, Miguel Alonso-Abella¹, Francisco J. Battles², Aitor Marzo⁴, Natalie Hanrieder⁵

5
6 ¹ Photovoltaic Solar Energy Unit (Energy Department, CIEMAT), Avda. Complutense 40, 28040
7 Madrid, Spain

8 ² Department of Chemistry and Physics, University of Almería, 04120, Almería, Spain

9 ³ Department of Electrical and Thermal Engineering, Design and Projects, University of Huelva,
10 21004, Huelva, Spain

11 ⁴ CDEA, University of Antofagasta, 02800, Antofagasta, Chile

12 ⁵ German Aerospace Center DLR, Institute of Solar Research, Paseo de Almería 73, 04001
13 Almería, Spain

14
15
16
17
18 * Corresponding author

19 Jesús Polo, email: jesus.polo@ciemat.es, Phone: +34 914962513

20 **Abstract**

21
22
23 Particle deposition on the surface of modules in PV systems produces energy output losses
24 with an impact that highly depends on the meteorological and climatic conditions. This work
25 presents the characterization of soiling losses for a suburban forest area in Madrid focused on
26 rooftop PV systems. The soiling loss measured in the testing system can reach around 6 %/day
27 for a tilt angle of 8° during summer. Models assessment is also presented and analyzed here
28 using two available soiling models from the well-known pvlib package. The use of the models is
29 not straightforward and some assumptions and recommendations are also presented in this
30 work to produce the best predictions. The applicability of physical models to suburban areas,
31 particularly in large cities in Europe, is remarked by the availability of air quality monitoring
32 ground stations. These results will enhance future studies on the potential impact of soiling in
33 European cities that will help to the distributed PV systems growth and penetration.

34
35
36 **Keywords:** PV modeling, Soiling losses, PV performance, Aerosols

37 38 39 **1. Introduction**

40
41
42 Photovoltaics penetration in the energy mix is growing faster and globally. However, the PV
43 landscape is foreseen to change, since while utility-scale PV systems have been dominating the

44 market, distributed PV systems are becoming more relevant in many countries [1]. Thus,
45 photovoltaic systems in buildings is an effective and sustainable means of producing
46 renewable energy on site [2]. Especially in urban areas, roof surfaces are increasingly
47 becoming PV roofs and improving the energy self-sufficiency of buildings, which helps the
48 reduction of the greenhouse gases emission in cities. While Building Integrated Photovoltaics
49 (BIPV) refers to the photovoltaic modules and systems substituting building components [3],
50 Building Applied Photovoltaics (BAPV) consists in the attachment of PV modules to existing
51 buildings. BIPV is the ideal solution for new buildings and retrofits [4], where PV modules play
52 a constructive role in façades or roofs, but BAPV can be an interesting alternative for existing
53 buildings not needing an envelope renovation. Both BAPV and simplified BIPV, using
54 conventional PV modules with dedicated mounting structures, have experienced positive
55 developments in numerous countries in 2019 [1].

56 The accumulation of dirt, dust, pollen and other environmental contaminants on the glazing
57 surfaces of the PV modules reduces the energy conversion efficiency due to the reduction of
58 the effective incoming irradiance. This effect, referred to as soiling, is a complex physical-
59 chemical phenomenon influenced by numerous factors acting on different size and time scales
60 and several models to estimate soiling losses can be found in the literature [5–7]. A thorough
61 overview of published PV soiling models until 2017 can be found in recent literature [8]. A
62 detailed revision of soiling can be found in the recent work of Isle et al. [9]; they provide an in-
63 depth understanding of the soiling processes, the role of the adhesion forces and self-cleaning
64 by wind under arid and semi-arid climatic conditions where soiling is mainly produced by
65 mineral dust. Although every PV system undergoes some energy loss due to soiling, PV
66 facilities running in areas exposed to high air concentrations of blown mineral dust, sea salt
67 mist or anthropogenic particulated pollutants become especially affected by soiling issues. For
68 instance, in Egypt, a 1-year-exposed dusty module and a 2-month-exposed dusty module
69 produced 35% and 25% less energy than a clean PV module, respectively [10] and in Saudi
70 Arabia, PV modules exhibited power output reductions of about 50% after being left unclean
71 for eight months and about 20% after a single dust storm event [11]. In comparison, the
72 performance loss due to long-term degradation processes would be of minor significance, with
73 power degradation annual rates of 1.08-1.22% being reported for crystalline silicon modules
74 after 25 years operating in hot dry deserts [12,13]. Thus, the degree of soiling has an important
75 impact on the yield assessment and so does the uncertainty in evaluating the typical soiling
76 losses [14].

77 When installed in buildings, the PV modules' position is constrained by the building geometry.
78 This frequently forces these PV modules to have tilts and orientations far from the optimal
79 ones, in contrast to the ground-level PV plants. One of the consequences of the varied
80 positions of modules in BIPV or BAPV systems is the different amount of soiling their surfaces
81 accumulate, which is strongly affected by the tilt angle and the distance of the PV modules to
82 the ground. Improving soiling forecasting would help to better decide on a suitable cleaning
83 schedule and to upgrade PV energy simulation models and tools, which should include the
84 impact of soiling as one of the causes of PV losses, named as soiling loss (*SL*) [9,15–21].
85 Although the influence of soiling on the PV performance has been extensively reported in the
86 literature, this work takes a further step towards assessing *SL* forecasting.

87 The modeling options for PV systems have spread with the availability and continuous
88 improvement of open-source or free tools. System Advisor Model (SAM) and pvlb are two of
89 the most widely used tools for modeling the performance of PV systems [22,23]. These models
90 estimate the efficiency reduction of the power output due to soiling by means of a derate
91 factor that reduces the effective irradiance. In the case of the pvlb package, there are a lot of
92 additional functions and models for dealing with different simulation steps, such as models for
93 solar irradiance, spectral effects, solar tracking and soiling [24,25]. These particular features
94 give great versatility to the pvlb package in modeling the performance of the PV systems.
95 However, the use of these additional models is not always straightforward and additional
96 knowledge and research are convenient for obtaining reliable results.

97 This work presents on the one hand the results of the soiling losses measured in both
98 commercial multi-crystalline silicon PV modules and glass coupons during one year of testing in
99 a rooftop site in a suburban area with nearby forest in Madrid (Spain). In addition, two PV
100 soiling models, which are included in pvlb, have been used to evaluate the modeling capability
101 against the experimental measurements. Daily soiling losses up to around 6% have been
102 observed during summer (after over 50 days without any precipitation) and about 2% during
103 winter. Finally, one of the main novelties in this work are, in addition to the soiling
104 experimental characterization, the lessons learned in the use of the models; particularly, the
105 relative influence and impact that some of their main input parameters have on soiling,
106 namely the deposition velocity of the airborne particles and the minimum amount of daily
107 rainfall to clean the modules (cleaning threshold), and the approaches for estimating them as
108 well. The capability of modeling the soiling from monitored particulate matter concentrations
109 is highly interesting for PV penetration in suburban and urban sites, since there are many cities
110 in Europe (like the Madrid case) with a network of air quality stations monitoring these
111 particles.

112 **2. Experimental setup**

113

114 Two different experimental approaches have been used for characterizing the soiling losses in
115 the PVCastSOIL project: an electrical setup that uses PV modules to explore the electrical loss
116 and a soiling test bench that exposes glass coupons to estimate the optical transmittance loss
117 underwent by the transparent covers of the nearby modules.

118

119 The experimental methodology for performing electrical measurements consists in the
120 comparative study of the performance of similar PV modules under the same working
121 conditions except soiling. The setup includes the PV modules under test and equipment to
122 measure different meteorological parameters and the I-V curves of each PV module. These
123 curves are taken for each module with a PVPM2540C (PVE Photovoltaik Engineering) I-V tracer
124 connected to a multiplexer, together with the PV module temperatures and the most relevant
125 meteorological variables. The electrical parameters such as the maximum power (P_{max}) and
126 the short-circuit current (I_{sc}) have been extracted from the I-V curves. The in-plane irradiance
127 has been measured with six crystalline silicon PV reference cells distributed along different
128 points of the planes of the PV arrays to serve for filtering data gathered under non-
129 homogeneous irradiance conditions. There are three multi-crystalline silicon PV modules at 8°

130 tilt and another three ones at 22° , all of them being south-oriented. At the beginning of each
131 monitoring period, all the PV modules were cleaned. Then, once a week only one of the two
132 modules per group (i.e. same tilt) was cleaned, serving as the two clean references. The so-
133 called PVCastSOIL testing facility is set at CIEMAT's headquarters in Madrid, Spain (latitude
134 40.41°N , Köppen climate type Csa), on the flat rooftop of a 10 m high building. Nearby, there is
135 a park area with conifer trees and there are also some paved roads, typical characteristics of
136 many residential areas in the surroundings of Madrid, where there are more green spaces and
137 less building density than in the city center. A picture of the small rooftop PV system used to
138 monitor the soiling losses at two different tilt angles at CIEMAT is shown in Figure 1.
139
140



141
142

143 Figure 1. Picture of the PVCastSOIL facility in the rooftop of one building at CIEMAT.
144

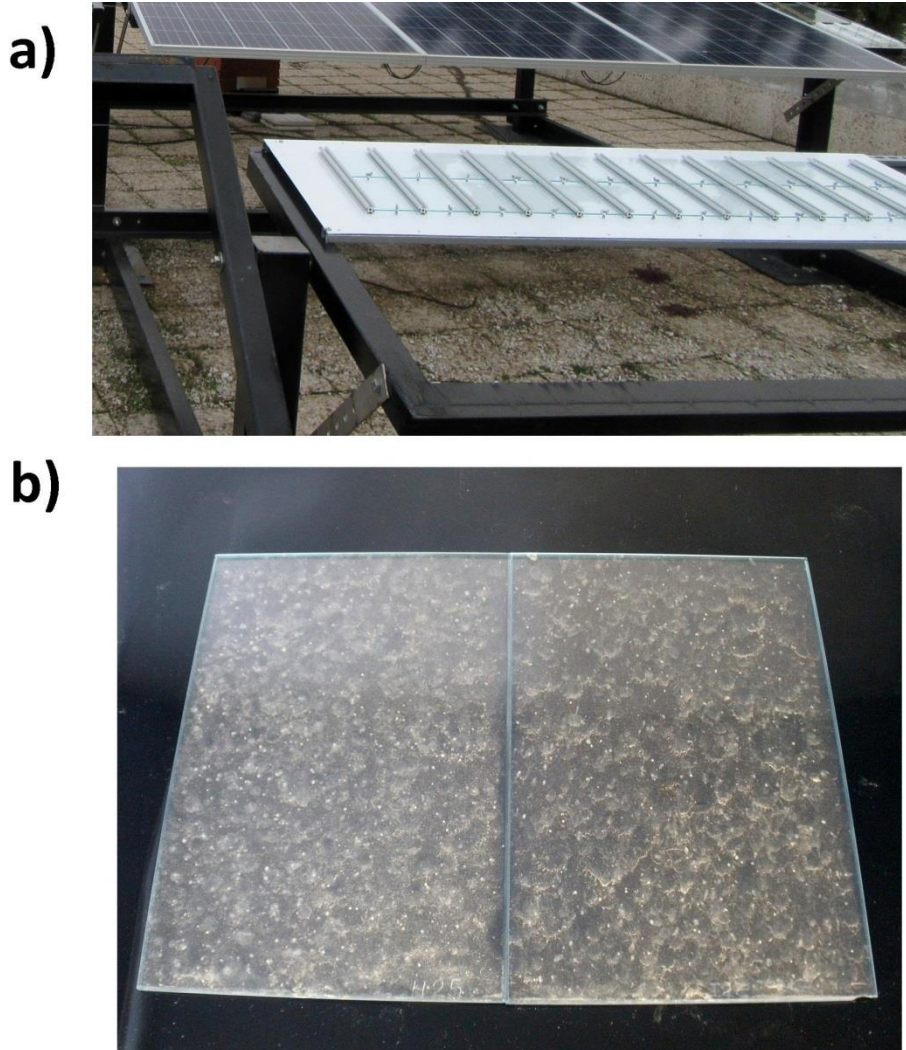
145 Concerning soiling monitoring through optical measurements, a soiling test bench was
146 installed to allow the long-term exposure of a large number of glass coupons. Soda lime glass
147 coupons of dimensions 10 cm x 15 cm were placed there and, as a general rule, the exposed
148 glass coupons were collected twice a week in order to characterize them optically in both
149 "dirty" and "clean" states. That is, the glass coupons were analyzed both after cleaning their
150 rear face with soft laboratory paper dampened with ethanol ("soiled coupons") and after
151 washing them with water and a soft sponge and letting them dry ("clean coupons").
152 Hemispherical transmittance measurements at near-normal incidence were performed using a
153 Perkin Elmer Lambda 900 UV/VIS/NIR spectrophotometer equipped with a 150-mm-diameter
154 integrating sphere. Hence, for each glass coupon, the optical soiling loss was derived by
155 measuring its "dirty state" transmittance spectrum (to account for non-homogeneous soiling
156 patterns, four measurements corresponding to four different sample points were averaged to

157 obtain a representative transmittance curve), normalizing it with respect to its “clean state”
158 transmittance spectrum, and finally averaging the transmittance value for the wavelength
159 interval from 340 nm to 1200 nm. Figure 2 shows a picture of the structure hosting the glass
160 coupons and an example of two soiled coupons.

161

162

163



164

165

166 Figure 2. Set of glass coupons for measuring the optical the soiling loss (a). Image of two soiled
167 glass coupons (b).

168

169 In addition to the electrical and optical measurements, standard meteorological
170 measurements (e.g. ambient temperature, relative humidity, wind speed and direction, and
171 rainfall) were collected both on the rooftop and in a nearby water tower behind the building.

172

173 Moreover, particle matter concentrations (PM_{2.5} and PM₁₀) have been measured in an air
174 quality station equipped with optical particle counters at CIEMAT. PM_{2.5} includes all particles
175 with diameters of less than 2.5 μm and, correspondingly, PM₁₀ includes those of less than
176 10 μm . The Madrid City Hall has a network of air quality stations whose data are openly
177 available. One station from this network (Casa de Campo) is placed about 5 km away from

178 CIEMAT in a similar forest environment; its data have been used to fill occasional gaps found in
179 the CIEMAT database of airborne particulate matter concentrations.

180

181

182 **3. Description of models for estimating the soiling ratio**

183

184 Two different models for estimating the soiling ratio, implemented in the pvlib tool, have been
185 analyzed and evaluated with the experimental measurements. First, the Kimber model [6] is a
186 very simple model that assumes a constant rate of soiling between two rainfall cleaning
187 events. The input to the model contains four main elements: the accumulated rainfall (mm),
188 the soiling rate, the cleaning threshold and the grace period length. The soiling rate is an
189 empirical parameter which refers to the fraction of energy loss per day. The cleaning threshold
190 is the minimum amount of daily rainfall required to clean the modules. Finally, the grace
191 period is the number of days assumed without significant soiling after a rainfall event.
192 Therefore, the Kimber model imposes a constant soiling rate after the grace period until the
193 next rain event reaching the cleaning threshold occurs. These parameters are purely empirical
194 and depend on both the geographical region and the soiling environment type; the authors
195 reported soiling rates from 0.1% in rural areas to 0.3% in suburban and urban ones [6].

196

197 Secondly, the HSU (Humboldt State University, CA USA) model relies on the assumption that
198 the soiling rate is determined by the accumulated rainfall (mm), the airborne particle matter
199 concentration (both $PM_{2.5}$ and PM_{10}) and the tilt angle of the exposed PV module [7]. Hence,
200 the soiling loss is calculated by,

201

$$202 \quad SL = 1 - 34.37 \operatorname{erf}(0.17 \omega^{0.8473}) \quad (1)$$

203

204

205 where ω is the total mass accumulation (g/m^2).

206

207 The total mass accumulation is the integral in time of the deposited mass rate,

208

209

$$210 \quad \omega = \int (v_{PM_{10}} C_{PM_{10}} + v_{PM_{2.5}} C_{PM_{2.5}}) \cos\beta \, dt \quad (2)$$

211

212

213 where $v_{PM_{10}}$ and $v_{PM_{2.5}}$ are the deposition velocities for airborne particles with aerodynamic
214 diameters less than 10 and 2.5 μm , respectively; $C_{PM_{10}}$ and $C_{PM_{2.5}}$ are the corresponding
215 mass concentrations of these airborne particles and β is the tilt angle of the PV module.

216

217 Likewise the Kimber model, the HSU model needs a cleaning threshold parameter to
218 determine the minimum accumulated rainfall required to completely clean the module.

219

220 The deposition velocities for airborne particles are affected by the wind speed, the particle
221 properties and size, and other factors that may make difficult to calculate theoretically [26].
222 The deposition velocities can be introduced in the HSU model as constants or can be calculated

223 as a function of the meteorological conditions (i.e. wind speed and ambient temperature)
 224 using the Zhang model for dry deposition velocity which is based on the Slinn's model
 225 developed for vegetated canopies [27,28]. In the HSU model implementation in pvlb it is
 226 recommended to use the gravitational settling velocity (0.0009 m/s and 0.004 m/s for PM_{2.5}
 227 and PM₁₀, respectively). However, it should be remarked that these values are significantly
 228 lower than dry deposition velocities reported in recent works for forest areas [29–31].
 229

230 4. Methodology for measuring the soiling loss

231

232 The soiling ratio, and thus the soiling loss, has been estimated here from a metric for
 233 performance index (PI_{ISC}) of the soiled and the reference modules. Since I-V curves are being
 234 continuously monitored in the experimental facility, the performance index computed for
 235 soiling estimations is calculated from the temperature-corrected short-circuit current. The
 236 short-circuit current of a PV module is proportional to the irradiance so that it seems to be the
 237 best parameter to characterize soiling losses, since soiling implies a reduction in the effective
 238 irradiance [32,33]. Therefore, the performance index computed from the short-circuit current
 239 is defined, in analogy with the performance ratio, as,
 240

241

242

$$PI_{ISC} = \frac{1000 I_{sc} (1 - \alpha_{SC}(T_{mod} - 25))}{I_{sc}^{STC} G_{POA}} \quad (3)$$

243

244

245 where I_{sc} and I_{sc}^{STC} are the short-circuit currents of the module at environmental
 246 conditions and at STC (Standard Test Conditions, 1000 W m⁻² and 25°C), respectively;
 247 α_{SC} is the temperature coefficient of the short-circuit current; T_{mod} is the module
 248 temperature; and G_{POA} is the plane of the array irradiance.
 249

250

251 Therefore the soiling loss (SL) can be defined from the corresponding performance
 252 index of the soiled (PI_{ISC}^{Soiled}) and reference modules (PI_{ISC}^{Clean}) as,
 253

254

255

$$SL = 1 - \frac{PI_{ISC}^{Soiled}}{PI_{ISC}^{Clean}} \quad (4)$$

256

257 The situation of the experimental facility (i.e. a rooftop with a few large trees nearby
 258 that shade the modules partially during the morning hours) somehow limits the
 259 computation of the daily soiling losses. Therefore, in order to avoid measurements
 260 with partial shading issues of the single modules, the daily soiling loss is computed by
 261 averaging the performance index of the instantaneous measurements in the time
 262 range of 12-18 hours (true solar times).

263 In the case of the optical measurements taken in the glass coupons the soiling loss is
 264 computed through the broadband transmittances of soiled (T_{Soiled}) and clean (T_{Clean})
 265 coupons by [34],

266

$$267 \quad SL = 1 - \frac{T_{Soiled}}{T_{Clean}} \quad (5)$$

268

269

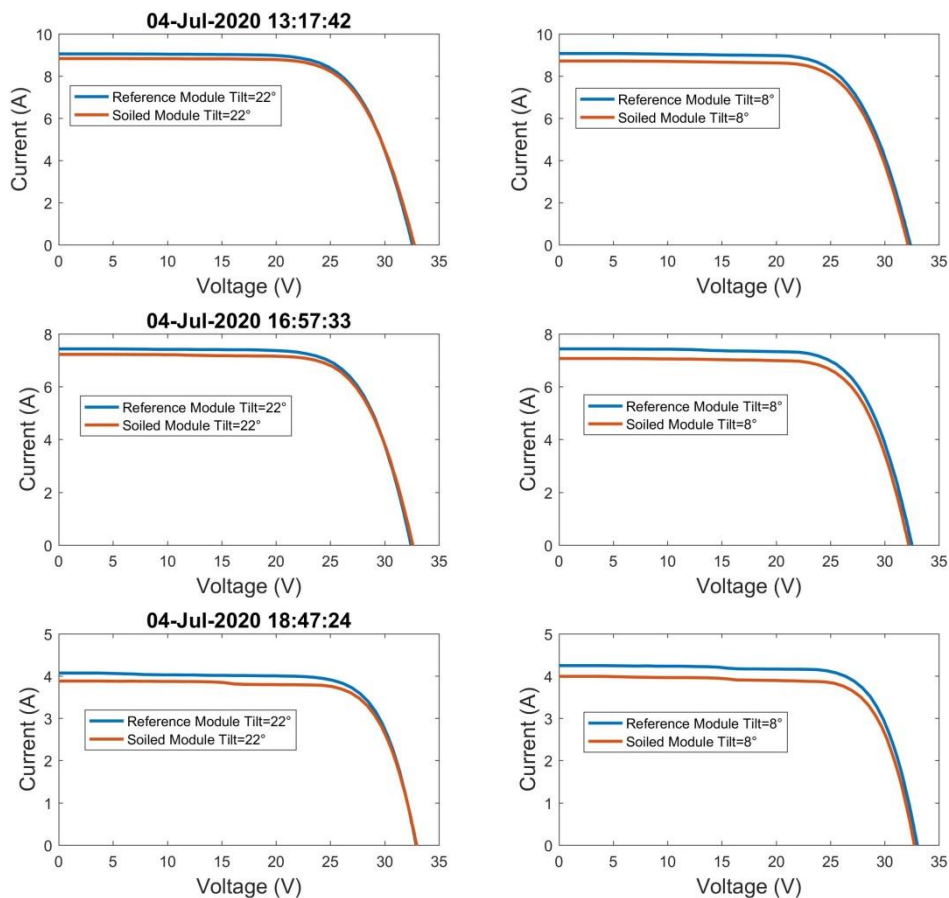
270 5. Results

271

272 The experimental campaign of soiling monitoring for silicon modules tilted 8° and 22° lasted
 273 from February 2019 until end of March 2021. Figure 3 shows the I-V curves of soiled and
 274 cleaned modules for three instantaneous measurements on 4th July 2020, namely during the
 275 dry summer season after many rainless days. The daily accumulated soiling loss for that day
 276 was 3.0% and 4.6% for tilt angles of 22° and 8° , respectively. It can be observed, that the losses
 277 are higher for the modules with lower tilt angles. Furthermore, it can be seen that for higher
 278 incidence angles (i.e. lower tilt angles) the soiling impact is higher.

279

280

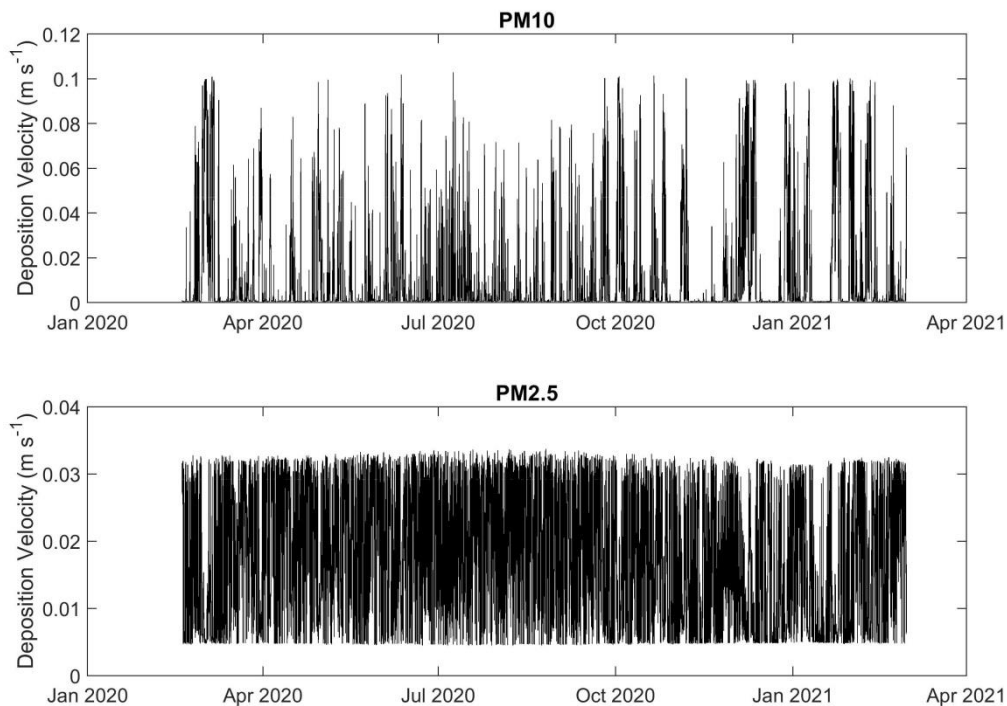


281

282 Figure 3. I-V curves of clean and soiled PV modules on July 4th, 2020.

283

284 Modeling the soiling loss with the HSU model requires some considerations regarding the
 285 deposition velocity. Deposition velocities for $PM_{2.5}$ and PM_{10} along the testing campaign (i.e.
 286 from February 2020 to March 2021) have been estimated with the Zhang model, implemented
 287 in pvlib, using as inputs the ambient temperature and the wind speed measured at CIEMAT
 288 and selecting evergreen land type. Figure 4 shows the resulting dry deposition velocities
 289 computed from the time series of ambient temperature and wind speed monitored at site.
 290 Larger variability in the velocities is observed for PM_{10} , which falls in the range 0.01-0.1 m/s,
 291 while the range of velocities for $PM_{2.5}$ is narrower (≈ 0.01 -0.03 m/s). These values are notably
 292 higher than the default settling velocities (0.0009 and 0.004 m/s for $PM_{2.5}$ and PM_{10} ,
 293 respectively). Modeling the deposition velocities has significant uncertainties [35]; however,
 294 these expected uncertainties do not completely explain the differences between the
 295 calculated dry deposition velocities for the test site and the default values from the HSU
 296 model. According to the variability and the range of values of the calculated deposition
 297 velocities it is expected a more realistic behavior of the HSU model using variable deposition
 298 velocities instead of constant default values.



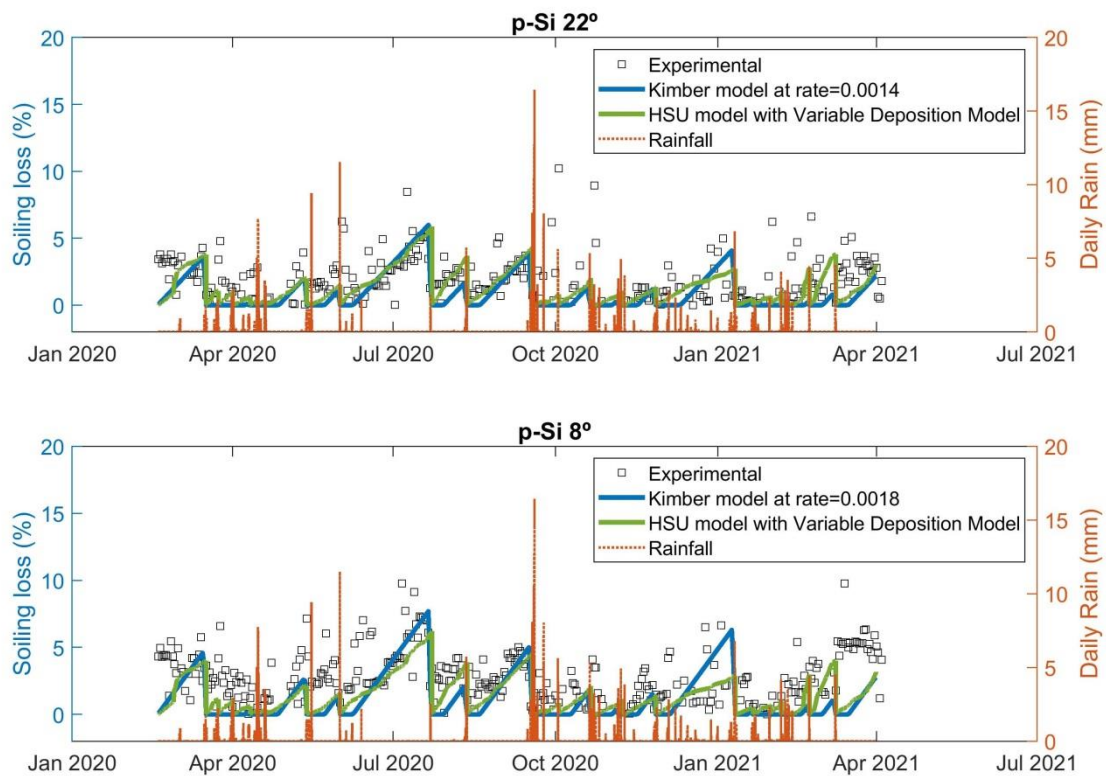
299

300 Figure 4. Calculated dry deposition velocities for $PM_{2.5}$ and PM_{10} estimated from ambient
 301 temperature and wind speed monitored at CIEMAT during the testing campaign using the
 302 model of Zhang et al., 2001.

303

304 Thus, soiling losses were modeled with the HSU model using the computed deposition
 305 velocities and a cleaning threshold of 4 mm. In addition, soiling losses have been also
 306 calculated with the Kimber model using purely empiric parameters. The daily soiling loss rate
 307 was set empirically to 0.0014 and 0.0018 for the 22° and 8° tilted modules, respectively. The
 308 default value recommended in the model implementation in pvlib is 0.0015. The cleaning
 309 threshold parameter (i.e. the minimum amount of daily rainfall required for fully cleaning) was

310 set to 4 mm as well. The grace period imposed in the Kimber model was 7 days, since the
 311 reference modules in the PVCastSOIL facility were cleaned every week, and such a value has
 312 been proposed in previous works [36]. Figure 5 presents the soiling losses estimated by the
 313 HSU and the Kimber models compared to the experimental measurements at the PVCastSOIL
 314 facility. A good agreement is generally found in both models. The chosen cleaning threshold of
 315 4 mm seems to fit quite well with the cleaning by rainfall observed in the experimental data,
 316 excepting for March 8th 2021 when 4.5 mm of measured rainfall did not result in complete
 317 cleaning of the modules. In that period the predicted trend of soiling of the HSU model was
 318 quite good compared with the experimental data but it dropped suddenly after the rainfall.
 319 This observation is more pronounced in the case of 8° tilt, since not all the rainfall events
 320 resulted in the complete cleaning of the modules.
 321
 322
 323



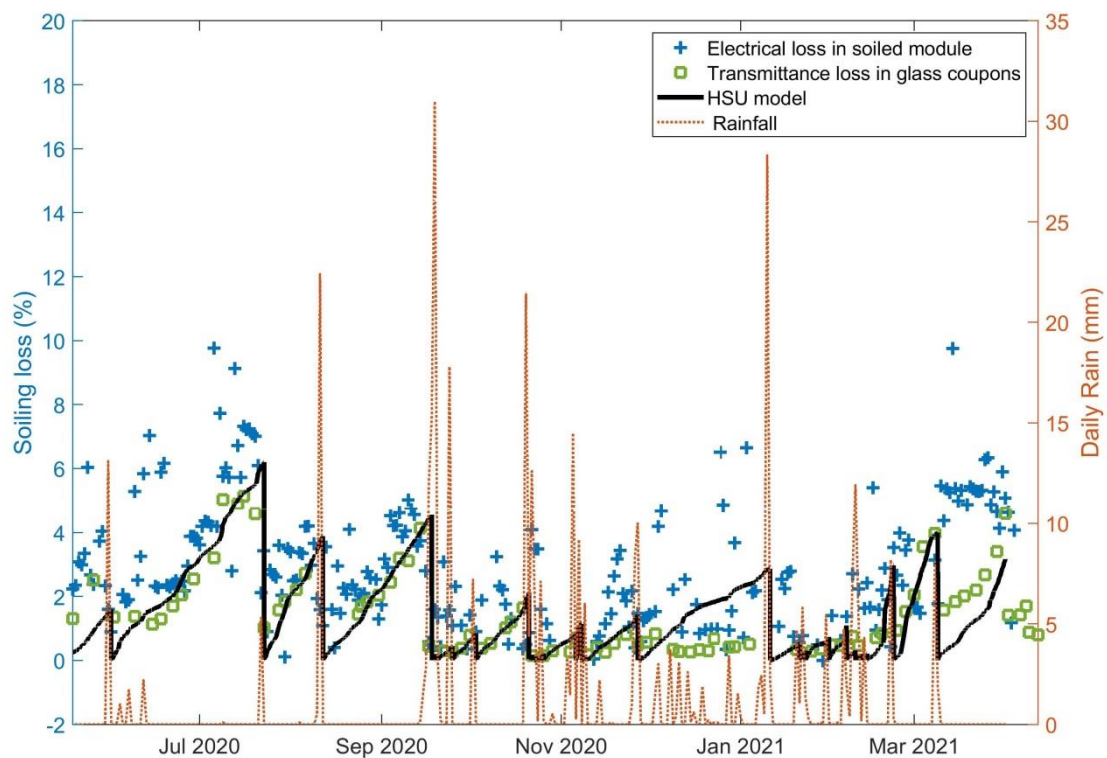
324
 325

326 Figure 5. Assessment of the HSU and the Kimber soiling models with the experimental soiling
 327 losses.

328
 329

330 Figure 6 shows the comparison of the electrical and optical soiling measurements with the HSU
 331 model estimations for the tilt angle 8°. In summer, with less frequent rainfall events registered,
 332 the measured daily soiling loss was around 6% and 4% after 52 and 38 days without rain,
 333 respectively. A general agreement and a correlation between the electrical and the optical
 334 soiling losses can be observed. However, the soiling measurements in the modules exhibit
 335 more dispersion than the optical ones, which follow a clearer and more continuous trend in

336 the periods between rainfall events. The agreement of the HSU model with the optical soiling
 337 losses in the summer season is remarkable. The larger discrepancies among them occur during
 338 periods with frequent rain events below the cleaning threshold (for instance, in December
 339 2020 and January 2021), highlighting the importance of tailoring the cleaning threshold
 340 parameter for a good modeling accuracy. On the other hand, a partial cleaning of the modules
 341 due to lower daily precipitation amounts is not contemplated by the model, which resets the
 342 soiling losses to zero whenever the cleaning threshold is reached, and it could be a limitation in
 343 the usage of the model depending on the local meteorology of the site.
 344
 345
 346



347
 348
 349 Figure 6. Comparison of electrical and optical soiling losses measured in the PVCastSOIL facility
 350 with the HSU model results for tilt=8°.
 351

352 6. Conclusions

353
 354 The impact of soiling losses in PV systems depends on the environmental and meteorological
 355 conditions of the emplacement. Proper characterization and modeling of the foreseen losses
 356 result in significant benefits that ease the penetration of PV systems and reduce the operating
 357 and maintenance costs. In the particular case of small rooftop systems the expected growth of
 358 distributed PV, particularly in urban and suburban areas of large cities in Europe, brings up the
 359 interest in the suitable characterization and knowledge of the soiling issue. In this work, one
 360 year of soiling losses measurements is analyzed for a small facility in a rooftop of a building in a

361 forest suburban area in Madrid. In addition, two available models are assessed with the
362 experimental data.

363

364 In modeling the soiling impact of a PV system under continental or temperate climatic
365 conditions, which typically results in moderate soiling compared to harsher conditions such as
366 in arid and desert environments, the cleaning threshold parameter plays a major role. This
367 parameter is mainly empirical. The observations in the experimental campaign and the results
368 of modeling the soiling loss have determined a value around 4-6 mm adequate for accurately
369 predicting the observations. The soiling models evaluated in this work were the Kimber model
370 (very simple and mostly empirical) and the HSU model (more detailed and including physical
371 fundamentals in its formulation). The former is limited to the previous input of the soiling rate,
372 which is stated constant and can be determined empirically from soiling observations. The
373 latter needs the particle matter concentration information as an input. Both models generally
374 showed good results to describe the experimental measurements, particularly in the summer
375 when the highest soiling losses were recorded (i.e. up to around 6 %/day).

376

377 The analysis of the models presented in this work remarks the need of a particular attention to
378 the deposition velocity. This is a relevant parameter in the HSU model that is variable and may
379 be largely affected by the meteorological conditions (especially by the wind speed). Under the
380 environmental conditions of the suburban area of Madrid the model of Zhang for estimating
381 variable deposition velocities for PM_{2.5} and PM₁₀ resulted in very good estimations of the
382 measured soiling loss. One of the main advantages of physical models, such as the HSU, is the
383 availability of using this model in suburban areas of cities in Europe since there are available
384 air quality stations that can provide particle matter concentration data needed by the model.
385 The work presented here has illustrated the use and the assumptions to be taken in available
386 soiling models, even the simplest ones, for rooftop PV applications.

387

388 **Acknowledgements**

389

390 The authors would like to thank the PVCastSOIL Project (ENE2017-469 83790-C3-1, 2 and 3),
391 which is funded by the Ministerio de Economía y Competitividad (MINECO), and co-financed by
392 the European Regional Development Fund. The authors also acknowledge
393 ANID/FONDAP/15110019 "Solar Energy Research Center" SERC-Chile; the Chilean Economic
394 Development Agency (CORFO) with contract No 17PTECES-75830 under the framework of the
395 project "AtaMoS TeC"; the generous financial support provided by GORE-Antofagasta, Chile,
396 Project FIC-R Antofagasta 2017 BIP code 30488824-0.

397

398

399 **References**

400

- 401 [1] Masson G, Kaizuka I, Bosch E, Detollenaere A, Neubourg G, van Wetter J, et al. IEA PVPS
402 report - Trends in Photovoltaic Applications 2020. 2020.
- 403 [2] Jäger-Waldau A. PV Status Report 2019. 2019. doi:10.2760/326629.

- 404 [3] Berger K, Cueli AB, Boddaert S, Del Buono S, Delisle V, Fedorova A, et al. International
405 definitions of “BIPV”. Report IEA-PVPS T15-04: 2018. International Energy Agency;
406 2018.
- 407 [4] Tjerk Reijenga, Ritzen M, Scognamiglio A, Kappel K, Frontini F, Moor D, et al. Successful
408 Building Integration of Photovoltaics - A collection of International Projects.
409 International Energy Agency; 2020.
- 410 [5] Toth S, Hannigan M, Vance M, Deceglie M. Predicting Photovoltaic Soiling From Air
411 Quality Measurements. *IEEE Journal of Photovoltaics* 2020;10:1142–7.
412 doi:10.1109/JPHOTOV.2020.2983990.
- 413 [6] Kimber A, Mitchell L, Nogradi S, Wenger H. The effect of soiling on large grid-connected
414 photovoltaic systems in California and the Southwest Region of the United States.
415 Conference Record of the 2006 IEEE 4th World Conference on Photovoltaic Energy
416 Conversion, WCPEC-4 2006;2:2391–5. doi:10.1109/WCPEC.2006.279690.
- 417 [7] Coello M, Boyle L. Simple Model for Predicting Time Series Soiling of Photovoltaic
418 Panels. *IEEE Journal of Photovoltaics* 2019;9:1382–7.
419 doi:10.1109/JPHOTOV.2019.2919628.
- 420 [8] Picotti G, Borghesani P, Cholette ME, Manzolini G. Soiling of solar collectors – Modelling
421 approaches for airborne dust and its interactions with surfaces. *Renewable and
422 Sustainable Energy Reviews* 2018;81:2343–57. doi:10.1016/j.rser.2017.06.043.
- 423 [9] Ilse KK, Figgis BW, Naumann V, Hagendorf C, Bagdahn J. Fundamentals of soiling
424 processes on photovoltaic modules. *Renewable and Sustainable Energy Reviews*
425 2018;98:239–54. doi:10.1016/j.rser.2018.09.015.
- 426 [10] Ibrahim M, Zinsser B, El-Sherif H, Hamouda E, Georghiou GE, Schubert MB, et al.
427 Advanced photovoltaic test park in Egypt for investigating the performance of different
428 module and cell technologies. *24 Symposium Photovoltaische Solarenergie* 2009:318–
429 23.
- 430 [11] Adinoyi MJ, Said SAM. Effect of dust accumulation on the power outputs of solar
431 photovoltaic modules. *Renewable Energy* 2013;60:633–6.
432 doi:10.1016/j.renene.2013.06.014.
- 433 [12] Bandou F, Hadj Arab A, Saïd Belkaid M, Logerais PO, Riou O, Charki A. Evaluation
434 performance of photovoltaic modules after a long time operation in Saharan
435 environment. *International Journal of Hydrogen Energy* 2015;40:13839–48.
436 doi:10.1016/j.ijhydene.2015.04.091.
- 437 [13] Tang Y, Raghuraman B, Kuitche J, TamizhMani G, Backus CE, Osterwald C. An evaluation
438 of 27+ years old photovoltaic modules operated in a hot-desert climatic condition.
439 Conference Record of the 2006 IEEE 4th World Conference on Photovoltaic Energy
440 Conversion, WCPEC-4, Waikoloa, HI, USA: 2007, p. 2145–7.
441 doi:10.1109/WCPEC.2006.279929.
- 442 [14] Moser D, Lindig S, Richter M, Asencio-Vasquez J, Horvath I, Müller B, et al. Uncertainties
443 in Yield Assessments and PV LCOE. Report IEA-PVPS T13-18:2020: 2020.
- 444 [15] Costa SCS, Sonia A, Diniz ASAC, Kazmerski LL. Dust and soiling issues and impacts
445 relating to solar energy systems: Literature review update for 2012-2015. *Renewable
446 and Sustainable Energy Reviews* 2016;63:33–61. doi:10.1016/j.rser.2016.04.059.

- 447 [16] Massi Pavan A, Mellit A, De Pieri D. The effect of soiling on energy production for large-
448 scale photovoltaic plants. *Solar Energy* 2011;85:1128–36.
449 doi:10.1016/J.SOLENER.2011.03.006.
- 450 [17] Maghami MR, Hizam H, Gomes C, Radzi MA, Rezadad MI, Hajighorbani S. Power loss
451 due to soiling on solar panel: A review. *Renewable and Sustainable Energy Reviews*
452 2016;59:1307–16. doi:10.1016/j.rser.2016.01.044.
- 453 [18] Appels R, Lefevre B, Herteleer B, Goverde H, Beerten A, Paesen R, et al. Effect of soiling
454 on photovoltaic modules. *Solar Energy* 2013;96:283–91.
455 doi:10.1016/j.solener.2013.07.017.
- 456 [19] Polo J, Martín-Chivelet N, Alonso M, Sanz C, Batlles FJ. Characterization of PV Soiling
457 Losses in Urban Mediterranean Environment. *ISES Solar World congress SWC/SHC*
458 2019, Santiago de Chile: 2020. doi:10.18086/swc.2019.15.03.
- 459 [20] John JJ. Characterization of Soiling Loss on Photovoltaic Modules , and Development of
460 a Novel Cleaning System. *Indian Institute of Technology Bombay*, 2015.
- 461 [21] Conceição R, Silva HG, Mirão J, Collares-Pereira M. Organic soiling: The role of pollen in
462 PV module performance degradation. *Energies* 2018. doi:10.3390/en11020294.
- 463 [22] F. Holmgren W, W. Hansen C, A. Mikofski M. Pvlb Python: a Python Package for
464 Modeling Solar Energy Systems. *Journal of Open Source Software* 2018;3:884.
465 doi:10.21105/joss.00884.
- 466 [23] Gurupira T, Rix AJ. PV Simulation Software Comparisons : Pvsyst , Nrel Sam and Pvlb.
467 *SAUPEC 2017*, 2017.
- 468 [24] Andrews RW, Stein JS, Hansen C, Riley D. Introduction to the open source pvlb for
469 python photovoltaic system modelling package. *40th IEEE Photovoltaic Specialist*
470 *Conference*, 2014.
- 471 [25] Holmgren WF, Andrews RW, Lorenzo AT, Stein JS. PVLIB Python 2015. *42nd*
472 *Photovoltaic Specialists Conference*, 2015.
- 473 [26] Boyle L, Flinchbaugh H, Hannigan M. Assessment of PM dry deposition on solar energy
474 harvesting systems: Measurement-model comparison. *Aerosol Science and Technology*
475 2016;50:380–91. doi:10.1080/02786826.2016.1153797.
- 476 [27] Zhang L, Gong S, Padro J, Barrie L. A size-segregated particle dry deposition scheme for
477 an atmospheric aerosol module. *Atmospheric Environment* 2001;35:549–60.
478 doi:10.1016/S1352-2310(00)00326-5.
- 479 [28] Slinn WGN. Predictions for particle deposition to vegetative canopies. *Atmospheric*
480 *Environment (1967)* 1982;16:1785–94. doi:10.1016/0004-6981(82)90271-2.
- 481 [29] Wu Y, Liu J, Zhai J, Cong L, Wang Y, Ma W, et al. Comparison of dry and wet deposition
482 of particulate matter in near-surface waters during summer. *PLoS ONE* 2018;13:1–15.
483 doi:10.1371/journal.pone.0199241.
- 484 [30] Zhu L, Liu J, Cong L, Ma W, Wu M, Zhang Z. Spatiotemporal characteristics of particulate
485 matter and dry deposition flux in the Cuihu Wetland of Beijing. *PLoS ONE* 2016;11:1–16.
486 doi:10.1371/journal.pone.0158616.

- 487 [31] Sun F, Yin Z, Lun X, Zhao Y, Li R, Shi F, et al. Deposition velocity of PM_{2.5} in the winter
488 and spring above deciduous and coniferous forests in Beijing, China. PLoS ONE
489 2014;9:1–11. doi:10.1371/journal.pone.0097723.
- 490 [32] Gostein M, Littmann B, Caron JR, Dunn L. Comparing PV power plant soiling
491 measurements extracted from PV module irradiance and power measurements. IEEE
492 39th Photovoltaic Specialists Conference, Tampa, FL, USA: 2013, p. 3004–9.
493 doi:10.1109/PVSC.2013.6745094.
- 494 [33] Simal-Pérez N, Alonso-Montesinos J, Batlles FJ. Estimation of soiling losses from an
495 experimental photovoltaic plant using artificial intelligence techniques. Applied
496 Sciences (Switzerland) 2021;11:1–18. doi:10.3390/app11041516.
- 497 [34] Sanz C, Polo J, Martín-Chivelet N. Influence of Pollen on Solar Photovoltaic Energy :
498 Literature Review and Experimental Testing with Pollen. Applied Sciences 2020;10:1–
499 25. doi:10.3390/app10144733.
- 500 [35] Saylor RD, Baker BD, Lee P, Tong D, Pan L, Hicks BB. The particle dry deposition
501 component of total deposition from air quality models: right, wrong or uncertain?
502 Tellus, Series B: Chemical and Physical Meteorology 2019;71:1–22.
503 doi:10.1080/16000889.2018.1550324.
- 504 [36] Deceglie MG, Micheli L, Muller M. Quantifying Soiling Loss Directly from PV Yield. IEEE
505 Journal of Photovoltaics 2018;8:547–51. doi:10.1109/JPHOTOV.2017.2784682.
- 506